Solution of the Boltzmann transport equation in an arbitrary one-dimensional-potential profile

M. M. Dignam and A. A. Grinberg
AT&T Bell Laboratories, Murray Hill, New Jersey 07974
(Received 20 October 1993)

We present a numerical approach to the solution of the Boltzmann transport equation in an arbitrary one-dimensional potential. Instead of employing the usual piecewise linear approximation to the potential in the discretization of the equation, we use a stepwise approximation. It is shown that due to absence of the electric field between mesh points, the Boltzmann transport equation can be reduced to a relatively simple equation involving only the spherical part of the distribution function. The method naturally describes situations where energy-band discontinuities take place—situations which are important in modern semiconductor heterostructures. We demonstrate the method for a system of finite length in a constant electric field. We observe a spatial periodicity in the electron drift velocity and average energy produced by interaction of electrons with optical phonons. These oscillations demonstrate one of the advantages of our method over Monte Carlo calculations, which do not predict such oscillations due to the averaging of the statistical data over distances larger than the oscillation period. We compare our results for the drift velocity in moderate electric fields (5 to 50 kV/cm) to a phenomenological model, finding the drift velocity to depend roughly on the square root of the field in this field range.

I. INTRODUCTION

The Boltzmann transport equation (BTE) in an arbitrary potential has not been analytically solved to date, even after employing considerably simplified particle scattering mechanisms. An exception is the solution of Mahan[1] for the BTE in a one-dimensional system (in both coordinate and momentum space), with energy-independent scattering via optical phonons. In its most complicated form, the BTE is a multidimensional, integrodifferential-difference equation, whose solution cannot be obtained, even by numerical methods, in all cases. The symmetry and homogeneity of a system can often result in a great reduction in the dimensionality of the BTE. The majority of work has been devoted to homogeneous systems in three-dimensional space in a constant electric field. Modern semiconductor device technology, however, requires the solution of the BTE in much more complex situations; typical high-speed semiconductor devices are not structurally homogeneous, and operate in spatially varying, large electric fields. For such systems, the Monte Carlo (MC) method[2] is often employed to solve the transport problem. However, it is by nature a stochastic method, and thus requires a large amount of computational time in order to obtain statistically reliable results. It is therefore very desirable to develop methods based on the direct numerical solution of the BTE. Although such methods are usually less general than the MC method, they are often useful in clarifying the basic principles of carrier transport.

The main difficulty in obtaining a solution to the BTE arises from its high dimensionality. Even for a potential which only varies in one dimension, the resulting BTE is a four-dimensional integrodifferential or integrodifferential-difference equation, which in its full generality usually requires the use of MC methods. A common technique employed to reduce the complexity of the BTE involves the expansion of the distribution function in some complete set of functions (usually spherical harmonic functions). The resulting infinite set of equations is then truncated using a criterion which depends upon the properties of the described system and the values of the relevant parameters.[1,3–5] In a recent work by Lin, Goldsman, and Mayergoyz,[6] such a method was applied to the solution of the BTE in an arbitrary potential profile. Although their method is numerically efficient, it is not applicable to systems in high electric fields, because they retain only the two first terms in the Legendre expansion of the distribution function.

As semiconductor structure growth technologies have progressed, practical problems have begun to require the solution of the BTE in more complicated situations. With the appearance of heterostructure devices, such as heterotransistors and hetero- or multiple-quantum-well lasers, it is necessary to solve the BTE not only in spatially varying electric fields, but in the presence of potential discontinuities as well.

The objective of this work is to present an approach to the numerical solution of the BTE in an arbitrary one-dimensional potential, which may include very high electric fields and potential discontinuities. The main restriction of our method is that the only scattering mechanisms that we can treat exactly are those which are isotropic. For semiconductors this means, first, that we are restricted to approximating the energy bands as being spherical, and, second, that we can only treat exactly scattering via acoustic and nonpolar optical phonons. The other scattering mechanisms, such as scattering from impurity centers or polar optical phonons, must be treated by using angular averaging of appropriate scattering cross sections.[7]

In order to examine our method in more detail, it is useful to look at the BTE in an arbitrary one-dimensional potential for parabolic and isotropic particle dispersion

$[E(\mathbf{k})=\hbar^2k^2/2m]$,

$$\frac{\partial f(z,\mathbf{k},t)}{\partial t}=-\frac{\hbar k_z}{m}\frac{\partial f(z,\mathbf{k},t)}{\partial z}-\frac{1}{\hbar}\frac{\partial U(z)}{\partial z}\frac{\partial f(z,\mathbf{k},t)}{\partial k_z}+\frac{\hbar k}{m}\{S^+[f(z,\mathbf{k},t)]-S^-[f(z,\mathbf{k},t)]\}\ , \tag{1.1}$$

where S^- and S^+ are the usual functionals describing the incoming and outgoing scattering rates of the particles, m is the effective particle mass, z is the coordinate in the direction of the electric field, $U(z)$ is the potential energy, and $\mathbf{k}$ is the particle wave vector. In what follows, we shall assume that nonpolar optical phonons provide the only inelastic particle scattering mechanism. If the spatial coordinates in the above integral equation are discretized (in order to reduce it to a matrix equation), the electric field in the intervals between mesh points is assumed constant. Thus, rather than employing the real potential [Fig. 1(a)], a piecewise linear potential [Fig. 1(b)] is used. If the BTE in a constant electric field could be partially integrated analytically and reduced to an equation with lower dimensionality, the numerical solution of the equation would be greatly simplified. As was shown by Baraff[8] and Keldysh,[9] in an infinite homogeneous system in a constant electric field, it is possible to reduce the steady-state form of this equation to an integral equation for the spherical part of distribution function, which is defined as

$$f^{(0)}(z,\mathbf{k},t)=\frac{1}{4\pi}\int f(z,\mathbf{k},t)d\Omega_k\ , \tag{1.2}$$

where Ω_k is the solid angle in $\mathbf{k}$ space. Unfortunately, such a method is not possible in a finite region where the distribution function is expected to vary spatially. However, a similar approach can be employed with the BTE in a finite region with zero electric field (constant potential). This is the central idea behind our approach; rather than using a piecewise linear potential [Fig. 1(b)] in the discretization of the BTE, we employ a *stepwise* potential [Fig. 1(c)]. It is clear that in the limit of an infinite density of mesh points, the results using either potential will be the same.

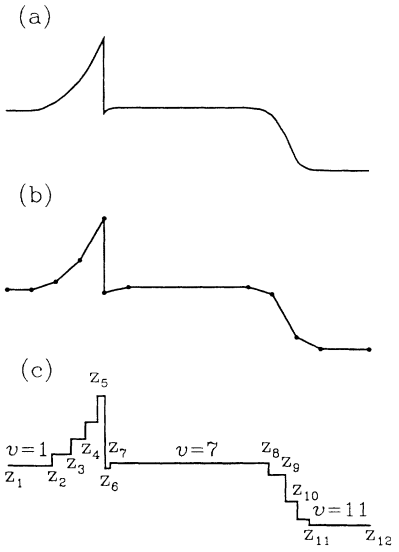

FIG. 1. Schematic illustration of the potential discretization: (a) a physical potential including discontinuities, (b) the commonly used piecewise linear approximation, and (c) the stepwise approximation employed in the present paper. The labels in (c) are included to aid in the description of the theory.

One principle advantage of our approach is that it deals naturally with potential discontinuities. If, for instance, the band-edge diagram has the form shown in Fig. 1(a), then with our method the discontinuity at $z=z_6$ [Fig. 1(c)] is taken into account automatically. In addition, we need only solve one integral equation in the entire $v=7$ interval, where the effective electric field is zero. The main disadvantage of the method is that we must provide boundary conditions consistent with introduced or physical potential discontinuities. This is the price we have to pay for the simplification of the equation.

In this work, we apply our method to calculate the velocity and energy dependence of electrons in a short interval ($\cong 0.2$ μm) in a constant electric field. The goal of this calculation is first to demonstrate the validity of our method by looking at results in a well-known system, and second to point out some interesting features of our results which have not been obtained using MC techniques.

The paper is organized as follows. In Sec. II we formulate the method of solution of the BTE in a finite interval with zero electric field. In Sec. III the boundary conditions connecting solutions in neighboring intervals are derived, and a set of coupled integral equations which describe the solution in a given interval is obtained. In Sec. IV we discuss the numerical method by which these equations are solved. In Sec. V the results for the velocities and energies in short regions of constant electric field are presented, and we propose a qualitative model of velocity-field behavior for fields of intermediate strength (5–50 kV/cm), which are below the field at which the velocity saturates. Finally, in Sec. VI the findings of this work are summarized.

II. FORMULATION OF THE SOLUTION IN ONE INTERVAL

The central feature of our method of solution of the BTE in an arbitrary one-dimensional potential profile is the dividing up of the structure into small intervals over which the potential is assumed constant (electric field is zero). The intervals are labeled by the index v ($v=1\rightarrow M$), and the positions of the left and right boundaries of the vth interval are denoted by z_v and z_{v+1} respectively [see Fig. 1(c)]. Taking the scattering parameters to be constant within each interval, the BTE in the vth interval can be written

$$\frac{\partial f_v(z,E_v,u_v,t)}{\partial t}=-\frac{\hbar k_z}{m}\frac{\partial f_v(z,E_v,u_v,t)}{\partial z}-\frac{\hbar k}{m}\frac{f_v(z,E_v,u_v,t)}{l_{\rm tot}(E_v)}+\frac{\hbar k}{m}S^+[f_v(z,E_v,u_v,t)]\ , \tag{2.1}$$

where $u_\nu \equiv k_z/k$ and E_ν is the kinetic energy of the electron in units of the optical phonon energy $\hbar\omega_{\rm op}$. The second term on the right side of Eq. (2.1) is the outgoing scattering term; this term can include not only processes of scattering but capture as well.

The total scattering length $l_{\rm tot}(E_\nu)$ which enters into Eq. (2.1) is given by

$$\frac{1}{l_{\rm tot}(E_\nu)}=\frac{1}{l_{\rm sc}(E_\nu)}+\frac{1}{l_{\rm cp}(E_\nu)}\ , \tag{2.2}$$

where $l_{\rm cp}(E_\nu)$ is the capture length associated with electron recombination and $l_{\rm sc}(E_\nu)$ is the scattering mean free path. In this work, we include scattering via charged impurities, acoustic phonons, and nonpolar optical phonons. Thus, the scattering length is given by

$$\frac{1}{l_{\rm sc}(E_\nu)}=\frac{1}{l_{\rm ac}^{\rm el}}+\frac{1}{l_{\rm imp}(E_\nu)}+\frac{1}{l_{\rm op}(E_\nu)}\ , \tag{2.3}$$

where (see Appendix A) $l_{\rm ac}^{\rm el}$ is the scattering length due to acoustic phonons in the quasielastic approximation, $l_{\rm imp}(E_\nu)$ is the scattering length due to charge impurity centers (with averaging over the solid-angle cross section of scattering[7]), and $l_{\rm op}(E_\nu)$ is the scattering length due to nonpolar optical phonons. The incoming scattering term can be written

$$\begin{aligned}S^+[f_\nu(z,E_\nu,u_\nu,t]=&A_0(E_\nu)f_\nu^{(0)}(z,E_\nu,t)\\&+A_+(E_\nu)f_\nu^{(0)}(z,E_\nu+1,t)\\&+A_-(E_\nu)f_\nu^{(0)}(z,E_\nu-1,t)\ ,\end{aligned} \tag{2.4}$$

where $f_\nu^{(0)}(z,E_\nu,t)$ is the symmetric part of the distribution function, defined as

$$f_\nu^{(0)}(z,E_\nu,t)=\frac{1}{2}\int_{-1}^{1}f_\nu(z,E_\nu,u_\nu,t)du_\nu\ , \tag{2.5}$$

and the coefficients $A_0(E_\nu)$, $A_+(E_\nu)$, and $A_-(E_\nu)$ are defined in Appendix A. It is seen that Eq. (2.4) involves only the symmetric part of the distribution function. This is the result of the spherical symmetry of the scattering cross section. From Eq. (2.4) it also follows that the distribution function at E_ν is directly connected to the distribution functions at $E_\nu\pm1$, making the BTE a finite-difference equation.

For the sake of generality, we consider a perturbation of the system which is periodic in time, and look for a solution of the form

$$f_\nu(z,E_\nu,u_\nu,t)=f_\nu(z,E_\nu,u_\nu)\exp(i\omega t)\ . \tag{2.6}$$

Due to the linearity of the BTE, the static solution can be found by simply setting $\omega=0$. Substituting (2.6) into (2.1) and factoring out the harmonic time dependence, we obtain

$$u_\nu\frac{\partial f_\nu(z,E_\nu,u_\nu)}{\partial z}+\frac{f_\nu(z,E_\nu,u_\nu)}{l_\nu^*}=R(z,E_\nu)\ , \tag{2.7}$$

where

$$R_\nu(z,E_\nu)\equiv S^+[f_\nu(z,E_\nu,u_\nu)]=S^+[f_\nu^{(0)}]\ ,$$

and

$$\frac{1}{l_\nu^*}\equiv\frac{i\omega m}{\hbar k}+\frac{1}{l_{\rm tot}(E_\nu)}\ . \tag{2.8}$$

Taking R_ν to be a free term in the differential equation, the general solution of the Boltzmann equation in the νth interval [Eq. (2.7)] can be written

$$\begin{aligned}f_\nu^{(+)}(z,E_\nu,u_\nu)=&f_\nu^{(+)}(z_\nu,E_\nu,u_\nu)\exp\left[-\frac{z-z_\nu}{u_\nu l_\nu^*}\right]\\&+\frac{1}{u_\nu}\int_{z_\nu}^{z}R_\nu(z',E_\nu)\exp\left[-\frac{z-z'}{u_\nu l_\nu^*}\right]dz'\ ,\end{aligned} \tag{2.9}$$

$$\begin{aligned}f_\nu^{(-)}(z,E_\nu,u_\nu)=&f_\nu^{(-)}(z_{\nu+1}E_\nu,u_\nu)\exp\left[-\frac{z-z_{\nu+1}}{u_\nu l_\nu^*}\right]\\&-\frac{1}{u_\nu}\int_{z}^{z_{\nu+1}}R_\nu(z',E_\nu)\\&\times\exp\left[-\frac{z-z'}{u_\nu l_\nu^*}\right]dz'\ ,\end{aligned} \tag{2.10}$$

where $f_\nu^{(+)}(z,E_\nu,u_\nu)$ [$f_\nu^{(-)}(z,E_\nu,u_\nu)$] is the portion of the distribution function for which $u_\nu>0$ ($u_\nu<0$). Because it is implicitly understood that $u_\nu<0$ in Eq. (2.10), it is convenient to redefine

$$f_\nu^{(-)}(z,E_\nu,u_\nu)\rightarrow f_\nu^{(-)}(z,E_\nu,-u_\nu)$$

and now take $u_\nu>0$ in $f_\nu^{(-)}(z,E_\nu,u_\nu)$. Thus Eq. (2.10) becomes

$$\begin{aligned}f_\nu^{(-)}(z,E_\nu,u_\nu)=&f_\nu^{(-)}(z_{\nu+1},E_\nu,u_\nu)\exp\left[-\frac{z_{\nu+1}-z}{u_\nu l_\nu^*}\right]\\&+\frac{1}{u_\nu}\int_{z}^{z_{\nu+1}}R_\nu(z',E_\nu)\\&\times\exp\left[-\frac{z'-z}{u_\nu l_\nu^*}\right]dz'\ .\end{aligned} \tag{2.11}$$

As they stand, the expressions for the half-space distribution functions, $f_\nu^{(\pm)}(z,E_\nu,u_\nu)$ [Eqs. (2.9) and (2.11)], depend upon the spherical portion of the distribution function in the νth interval, and upon the half-space distribution functions $f_\nu^{(-)}(z_{\nu+1},E_\nu,u_\nu)$ and $f_\nu^{(+)}(z_\nu,E_\nu,u_\nu)$ evaluated just *inside* the two boundaries of the νth interval. In order to solve the problem in the complete structure, it is necessary to relate the solution in the νth interval to the solutions in the neighboring intervals. To accomplish this, we therefore need to obtain expressions for $f_\nu^{(-)}(z_{\nu+1},E_\nu,u_\nu)$ and $f_\nu^{(+)}(z_\nu,E_\nu,u_\nu)$ in terms of the incoming distribution functions, $f_{\nu-1}^{(+)}(z_\nu,E_{\nu-1},u_{\nu-1})$ and $f_{\nu+1}^{(-)}(z_{\nu+1},E_{\nu+1},u_{\nu+1})$ in the *neighboring* intervals. This is addressed in the following section.

III. SOLUTION INCLUDING THE BOUNDARY CONDITIONS

In this section, we derive boundary conditions for a given interval and use these boundary conditions to reduce Eqs. (2.9) and (2.11) to a single integral equation for the spherical part of the distribution function. As shown in Fig. 1(c), the true potential $U(z)$ is approximated by a stepwise potential which takes the value U_ν over the νth interval. The height Δ_ν of the step in this potential at the point z_ν is defined as

$$\Delta_\nu \equiv U_{\nu+1} - U_\nu \ , \tag{3.1}$$

yielding a Δ_ν which is negative when the potential energy decreases with increasing z. In what follows we neglect the discontinuity in effective mass which occurs across real potential discontinuities at heterointerfaces. Such a generalization is straightforward but for the sake of simplicity of presentation is not included here.

Let us consider the boundary conditions at the interface z_ν. The electrons entering from region $\nu-1$ into region ν abruptly change their kinetic energy by the magnitude of the potential discontinuity, $-\Delta_\nu$. The boundary condition must ensure continuity of the differential flux at the interface, i.e., the flux of the electrons with wave vectors located in the three-dimensional volume $d^3\mathbf{k}_{\nu-1}$ on the left side of the interface must be equal to the flux of the electrons with wave vectors located in some volume $d^3\mathbf{k}_\nu$ on the right side. Consider first the part of the distribution function $f(z,E,u)$ which contributes to the positive particle flux ($u_{\nu-1}, u_\nu \geq 0$). The differential particle flux on the left side of the interface is given by

$$dJ_{\nu-1}(z_\nu - 0_+) = \frac{2}{(2\pi)^3}\frac{\hbar k_{\nu-1,z}}{m} \times f_{\nu-1}^{(+)}(z_\nu - 0_+, E_{\nu-1}, u_{\nu-1}) \times d^2\mathbf{k}_{\nu-1,\parallel} dk_{\nu-1,z} \ . \tag{3.2a}$$

Analogously, the particle flux on the right side is

$$dJ_\nu(z_\nu + 0_+) = \frac{2}{(2\pi)^3}\frac{\hbar k_{\nu,z}}{m} f_\nu^{(+)}(z_\nu + 0_+, E_\nu, u_\nu) \times d^2\mathbf{k}_{\nu,\parallel} dk_{\nu,z} \ , \tag{3.2b}$$

where $\mathbf{k}_{\nu,\parallel}$ is the component of the wave vector parallel to the interface. Sine this component does not change when an electron crosses the interface, we have the equality $d^2\mathbf{k}_{\nu,\parallel} = d^2\mathbf{k}_{\nu-1,\parallel}$. In addition, there exists the relation

$$k_{\nu,z} dk_{\nu,z} = k_{\nu-1,z} dk_{\nu-1,z} \ ,$$

which follows from the energy conservation law

$$E_\nu = E_{\nu-1} - \Delta_\nu \ . \tag{3.3}$$

Using the definitions of $u_{\nu-1}$ and u_ν, and employing Eq. (3.3), the relation between the wave-vector cosines in the two intervals is found to be

$$u_{\nu-1} \equiv \gamma_\nu^- = \left[\frac{E_\nu u_\nu^2 + \Delta_\nu}{E_\nu + \Delta_\nu}\right]^{1/2} \quad \text{if } u_\nu^- < u_\nu < 1 \ , \tag{3.4}$$

where

$$u_\nu^- = \begin{cases} 0 & \text{if } \Delta_\nu \geq 0 \\ [-\Delta_\nu/E_\nu]^{1/2} & \text{if } -\Delta_\nu < E_\nu \\ 1 & \text{if } -\Delta_\nu \geq E_\nu \ . \end{cases} \tag{3.5}$$

Thus, from Eq. (3.2) and the conservation laws, it follows that

$$f_\nu^{(+)}(z_\nu, E_\nu, u_\nu) = f_{\nu-1}^{(+)}\left[z_\nu, E_\nu + \Delta_\nu, \left[\frac{E_\nu u_\nu^2 + \Delta_\nu}{E_\nu + \Delta_\nu}\right]^{1/2}\right] \quad \text{if } u_\nu > u_\nu^- \ . \tag{3.6}$$

The physical explanation of the inequality involving u_ν in Eq. (3.6) is that if an electron is to penetrate into the region ν from region $\nu-1$ it must have a z component of the momentum, $\hbar k_z$, larger than $\sqrt{-2m\Delta_\nu}$. The Eq. (3.6) determines the distribution function $f_\nu^{(+)}(z_\nu)$ only for angles and energies which are consistent with the inequality $u_\nu^- < u_\nu < 1$. Electrons with z component of the momentum less than $\sqrt{-2m\Delta_\nu}$ undergo specular refection, and the appropriate boundary condition is

$$f_\nu^{(+)}(z_\nu, E_\nu, u_\nu) = f_\nu^{(-)}(z_\nu, E_\nu, u_\nu) \quad \text{if } u_\nu < u_\nu^- \ . \tag{3.7}$$

We note that because $u_\nu > 0$, if $\Delta_\nu \geq 0$, there is no energy interval where the inequality in Eq. (3.7) can be satisfied. Equations (3.6) and (3.7) can be written in more compact form as

$$f_\nu^{(+)}(z_\nu, E_\nu, u_\nu) = \theta(\xi_\nu^-) f_{\nu-1}^{(+)}(z_\nu, E_\nu + \Delta_\nu, \gamma_\nu^-) + \theta(-\xi_\nu^-) f_\nu^{(-)}(z_\nu, E_\nu, u_\nu) \ , \tag{3.8}$$

where

$$\xi_\nu^- \equiv E_\nu u_\nu^2 + \Delta_\nu \ , \tag{3.9}$$

and $\theta(x)$ is the Heaviside step function.

Similarly, the appropriate boundary condition on the right side of region ν for the distribution function with negative k_z is found to be

$$f_\nu^{(-)}(z_{\nu+1}, E_\nu, u_\nu) = \theta(\xi_\nu^+) f_{\nu+1}^{(-)}(z_{\nu+1}, E_\nu - \Delta_{\nu+1}, \gamma_\nu^+) + \theta(-\xi_\nu^+) f_\nu^{(+)}(z_{\nu+1}, E_\nu, u_\nu) \ , \tag{3.10}$$

where

$$\gamma_\nu^+ \equiv \left[\frac{E_\nu u_\nu^2 - \Delta_{\nu+1}}{E_\nu - \Delta_{\nu+1}}\right]^{1/2} \quad \text{if } u_\nu^+ < u_\nu < 1 \ , \tag{3.11}$$

$$u_\nu^+ = \begin{cases} 0 & \text{if } \Delta_{\nu+1} \leq 0 \\ [\Delta_{\nu+1}/E_\nu]^{1/2} & \text{if } \Delta_{\nu+1} < E_\nu \\ 1 & \text{if } \Delta_{\nu+1} \geq E_\nu \ , \end{cases} \tag{3.12}$$

and

$$\xi_\nu^+ \equiv E_\nu u_\nu^2 - \Delta_{\nu+1} \ . \tag{3.13}$$

Using Eqs. (3.8) and (3.10) in Eqs. (2.9) and (2.11) in order to eliminate $f_\nu^{(+)}(z_\nu, E_\nu, u_\nu)$ and $f_\nu^{(-)}(z_{\nu+1}, E_\nu, u_\nu)$,

we obtain

$$f_\nu^{(+)}(z,E_\nu,u_\nu)=\exp\left[-\frac{z-z_\nu}{u_\nu l_\nu^*}\right]\left\{\theta(\xi_\nu^-)f_{\nu-1}^{(+)}(z_\nu,E_\nu+\Delta_\nu,\gamma_\nu^-)+\frac{1}{u_\nu}\int_{z_\nu}^{z}R_\nu(z',E_\nu)\exp\left[-\frac{z_\nu-z'}{u_\nu l_\nu^*}\right]dz'\right.$$
$$+\theta(-\xi_\nu^-)\theta(\xi_\nu^+)\left[f_{\nu+1}^{(-)}(z_{\nu+1},E_\nu-\Delta_{\nu+1},\gamma_\nu^+)\exp\left[-\frac{w_\nu}{u_\nu l_\nu^*}\right]\right.$$
$$\left.+\frac{1}{u_\nu}\int_{z_\nu}^{z_{\nu+1}}R_\nu(z',E_\nu)\exp\left[-\frac{z'-z_\nu}{u_\nu l_\nu^*}\right]dz'\right]$$
$$\left.+\frac{\theta(-\xi_\nu^-)\theta(-\xi_\nu^+)}{u_\nu\sinh(w_\nu/u_\nu l_\nu^*)}\int_{z_\nu}^{z_{\nu+1}}R_\nu(z',E_\nu)\cosh\left[\frac{z_{\nu+1}-z'}{u_\nu l_\nu^*}\right]dz'\right\},\tag{3.14a}$$

and

$$f_\nu^{(-)}(z,E_\nu,u_\nu)=\exp\left[\frac{z-z_{\nu+1}}{u_\nu l_\nu^*}\right]\left\{\theta(\xi_\nu^+)f_{\nu+1}^{(-)}(z_{\nu+1},E_\nu-\Delta_{\nu+1},\gamma_\nu^+)+\frac{1}{u_\nu}\int_{z}^{z_{\nu+1}}R_\nu(z',E_\nu)\exp\left[\frac{z_{\nu+1}-z'}{u_\nu l_\nu^*}\right]dz'\right.$$
$$+\theta(-\xi_\nu^+)\theta(\xi_\nu^-)\left[f_{\nu-1}^{(+)}(z_\nu,E_\nu+\Delta_\nu,\gamma_\nu^-)\exp\left[-\frac{w_\nu}{u_\nu l_\nu^*}\right]\right.$$
$$\left.+\frac{1}{u_\nu}\int_{z_\nu}^{z_{\nu+1}}R_\nu(z',E_\nu)\exp\left[\frac{z'-z_{\nu+1}}{u_\nu l_\nu^*}\right]dz'\right]$$
$$\left.-\frac{\theta(-\xi_\nu^+)\theta(-\xi_\nu^-)}{u_\nu\sinh(w_\nu/u_\nu l_\nu^*)}\int_{z_\nu}^{z_{\nu+1}}R_\nu(z',E_\nu)\cosh\left[\frac{z_\nu-z'}{u_\nu l_\nu^*}\right]dz'\right\}.\tag{3.14b}$$

Integrating the expressions for the half-space distribution functions [Eqs. (3.14)] over u_ν and adding the results together yields the following integral equation for the spherical part of the distribution function:

$$f_\nu^{(0)}(z,E_\nu)=\frac{1}{2}\left\{\int_{z_\nu}^{z_{\nu+1}}K_\nu(z,z',E_\nu)R_\nu(z',E_\nu)dz'\right.$$
$$+\int_{u_\nu^-}^{1}f_{\nu-1}^{(+)}(z_\nu,E_\nu+\Delta_\nu,\gamma_\nu^-)\exp\left[-\frac{w_\nu}{u_\nu l_\nu^*}\right]\left[\exp\left[-\frac{z-z_{\nu+1}}{u_\nu l_\nu^*}\right]+\theta(u_\nu^+-u_\nu^-)\exp\left[\frac{z-z_{\nu+1}}{u_\nu l_\nu^*}\right]\right]du_\nu$$
$$+\int_{u_\nu^+}^{1}f_{\nu+1}^{(-)}(z_{\nu+1},E_\nu-\Delta_{\nu+1},\gamma_\nu^+)\exp\left[-\frac{w_\nu}{u_\nu l_\nu^*}\right]$$
$$\left.\times\left[\exp\left[-\frac{z_\nu-z}{u_\nu l_\nu^*}\right]+\theta(u_\nu^--u_\nu^+)\exp\left[\frac{z_\nu-z}{u_\nu l_\nu^*}\right]\right]du_\nu\right\},\tag{3.15}$$

where $K_\nu(z,z',E_\nu)$ is the kernel which is given explicitly in Appendix B, and $\omega_\nu=Z_{\nu+1}-Z_\nu$.

Finally, the expression for the current density is given by

$$J_\nu(z)=-\frac{2e}{(2\pi)^3}\int\frac{\hbar\mathbf{k}}{m}f_\nu(z,E_\nu,u_\nu)d^3\mathbf{k}$$
$$=-\frac{em}{\pi^2\hbar^3}\int_0^\infty E_\nu dE_\nu\int_0^1 du_\nu u_\nu[f_\nu^{(+)}(z,E_\nu,u_\nu)-f_\nu^{(-)}(z,E_\nu,u_\nu)]\,.\tag{3.16}$$

This expression can be further simplified using Eq. (3.14) to yield an expression involving only the spherical distribution function and the distribution function at the two boundaries; as this expression is rather complicated we do not present it here.

IV. METHOD OF NUMERICAL SOLUTION

Once the boundary conditions for a given interval are known, the problem is reduced to solving Eq. (3.15) for the spherical part of the distribution function. From this the full distribution function can be calculated at any point z, using Eqs. (3.14), and the current density can then be calculated using Eq. (3.16).

Equation (3.15) represents a set of coupled integral equations, with coupling occurring only between those distribution functions $f_\nu^{(0)}$ which are separated in energy by an integral number of optical phonon energies, i.e., energies which take the form $E_\nu^n=\varepsilon_\nu+n$, where

$\varepsilon_\nu \equiv \mathrm{mod}[E_\nu]_1$. The numerical solution is thus obtained by discretizing the integration variable z' on a uniform grid Z_i, $i=\{1\cdots N_\nu\}$ and inverting the resulting matrix equation. In discretized form, the set of coupled integral equations represented by Eq. (3.15) can be written

$$\mathbf{F}(\varepsilon_\nu)=\overleftrightarrow{M}(\varepsilon_\nu)\cdot\mathbf{F}(\varepsilon_\nu)+\mathbf{G}(\varepsilon_\nu)\ , \tag{4.1}$$

where $\mathbf{F}(\varepsilon_\nu)$ and $\mathbf{G}(\varepsilon_\nu)$ are vectors with components labeled by the indices i and n, where i labels the spatial position Z_i, and n labels the energy E_ν^n. Thus $[\mathbf{F}(\varepsilon_\nu)]_{(in)}\equiv f_\nu^{(0)}(Z_i,\varepsilon_\nu+n)$, and $\mathbf{G}(\varepsilon_\nu)$ is a vector with the (in)th component given by the sum of the second and third terms on the right of Eq. (3.15) evaluated at $z=Z_i$ and $E_\nu=\varepsilon_\nu+n$. The matrix $\overleftrightarrow{M}(\varepsilon_\nu)$ is block tridiagonal, with block dimension N_ν, and elements given by

$$[\overleftrightarrow{M}(\varepsilon_\nu)]_{(in),(jm)}\equiv K_\nu(Z_i,Z_j,\varepsilon_\nu+n)\times\sum_{\sigma=-1}^{1}\delta_{n,m+\sigma}A_\sigma(\varepsilon_\nu+n)\ . \tag{4.2}$$

For a given value of ε_ν, Eq. (4.1) represents an infinite set of coupled vector equations, one equation for each value of the kinetic energy $E_\nu^n, n=\{0,1,\ldots\}$. In practice, one truncates the values of n to include in $\mathbf{F}(\varepsilon_\nu)$ only those components for which E_ν^n is no more than a few k_BT larger than the maximum value of $U(z)$. Typically, the matrices involved are relatively small ($\lesssim 100\times 100$), and so it is a simple matter to invert the matrices numerically. The only complication lies in the fact that $K_\nu(Z_i,Z_j,E_\nu)$ is singular for $i=j$. This singularity can be handled using standard techniques (see Appendix B). Thus, for a given ε_ν, the solution in a particular interval is found by inverting Eq. (4.1) to solve for $\mathbf{F}(\varepsilon_\nu)$. The solution at all energies is obtained to arbitrary accuracy by forming a grid in ε_ν from $0\rightarrow 1$. In practice, one needs only 10–20 energy grid points for the steady-state problem. For the time-dependent problem at very high frequencies, however, $f_\nu^{(0)}(E_\nu)$ is a very rapidly varying function of E_ν and a finer grid is necessary.

In order to solve Eq. (4.1) for a given interval ν, we need the incoming distribution function at both ends of the interval. However, in general, we only know the incoming portions of the distribution function on either side of the *entire structure*. The solution must therefore proceed via an iterative scheme. If we have obtained the solution in the $\nu-1$ interval, then when solving Eq. (4.1) in the ν interval, we know $f_{\nu-1}^{(+)}(z_\nu,E_{\nu-1},u_{\nu-1})$, but we do not know $f_{\nu+1}^{(-)}(z_{\nu+1},E_{\nu+1},u_{\nu+1})$. It is necessary, therefore, to obtain an approximate solution in this region by employing an initial guess for $f_{\nu+1}^{(-)}(z_{\nu+1},E_{\nu+1},u_{\nu+1})$ (usually setting it to zero). Using this method, we can proceed along the whole structure, finding provisional solutions in each interval. We then loop through all of the intervals repeatedly until the solution in each region converges. In practice, we find it sufficient to iterate until the current at a few selected points converges, which typically requires fewer than five iterations. Because the matrix $\overleftrightarrow{M}(\varepsilon_\nu)$ is independent of $\mathbf{G}(\varepsilon_\nu)$, it can be evaluated and inverted on the first iteration and the inverted matrix can be used in latter iterations, thereby saving computational time.

V. RESULTS

In this section, we describe the application of our method to the problem of electron transport through a short region of constant electric field. The distribution function entering the left of the field region is taken to be in thermal equilibrium and is given by

$$f_0^{(+)}(z_1,E_0,u_0)=e^{-E_0/k_BT}\ . \tag{5.1}$$

In order to achieve rapid numerical convergence, the right boundary of the structure is taken to be totally absorbing, i.e., $f_{M+1}^{(-)}(z_N,E_N,u_N)=0$. This boundary condition only affects the calculated results appreciably within a distance $k_BT/(eF)$ ($\leq 0.02\,\mu$m for $F\geq 5$ kV/cm) of the right boundary of the structure. The temperature was chosen to be 10 meV to ensure that the vast majority of the electrons entering the electric field region have a kinetic energy which is less than the optical phonon energy, $\hbar\omega_{\mathrm{op}}\cong 51.7$ meV. This is not essential for obtaining a solution, but it simplifies the interpretation of the results. The length of the field region W is $0.2\,\mu$m. The parameters used in scattering cross sections are those appropriate to Si, and are given in Table I.

TABLE I. The material parameters used to calculate the scattering matrix elements of silicon in the BTE calculations. The symbol m_0 refers to the free-electron mass.

Parameter	Notation	Value
Lattice temperature	k_BT	10 meV
Electron effective mass	m	$0.31m_0$
Acoustic deformation potential	E_{ac}	7.0 eV
Optical deformation potential	E_{op}	17.84 eV
Low-frequency dielectric constant	ε_0	11.7
Impurity (donor) concentration	N_i	5×10^{17} cm^{-3}
Material density	ρ	2.33 g cm^{-3}
Sound velocity	S	9.04×10^5 cm s^{-1}
Optical phonon energy	$\hbar\omega_{\mathrm{op}}$	51.7 meV
Effective optic free path [Eq. (A2)]	l_{op}	2.71×10^{-6} cm
Acoustic free path [Eq. (A3)]	$l_{\mathrm{ac}}^{\mathrm{el}}$	4.60×10^{-5} cm
Screening length [Eq. (A6)]	L_D	2.927×10^{-7} cm

In Fig. 2 we present the results for the steady-state velocity in the z direction as a function of z for four different electric field values. The region is broken up into 40–60 intervals, depending upon the electric field strength. Because the current is constant, the electron concentration abruptly changes at the points z_ν where the artificial potential discontinuities have been introduced. In order to smooth out the velocity discontinuities associated with these density discontinuities, the velocities plotted in Fig. 2 are obtained by averaging over each of the intervals. Thus, the average velocity $\bar{v}_\nu(\bar{z}_\nu)$, in each interval is defined as

$$v_z(\bar{z}_\nu) \equiv \frac{Jw_\nu}{\int_{z_\nu}^{z_{\nu+1}} n_\nu(z)dz} , \tag{5.2}$$

where J is the current density (which is constant throughout the structure), $\bar{z}_\nu$ is the center of the νth interval, and w_ν is its width.

For all four values of electric field used, oscillations in the velocity are observed as a function of the distance. These oscillations occur over distances greater than the potential discretization lengths and have nothing to do with the artificial potential discontinuities. It is clear that the source of these oscillations is optical phonon emission. When electrons enter the field region, they initially accelerate, and the average velocity goes up. At some point, when their energy exceeds $\hbar\omega_{op}$, they can emit an optical phonon; when a significant number of electrons have emitted optical phonons, the average velocity begins to decrease. This continues until even the electrons which initially had the lowest kinetic energy can also emit an optical phonon. Past this point, the kinetic energy gained by the electric field overcomes, on average, the energy lost due to phonon emission, and the velocity increases again. This process is repeated a number of times, resulting in the observed oscillations of period $L_{op} \equiv \hbar\omega_{op}/eF$. The amplitude of these oscillations is dependent upon the ratio of this oscillation period to the optical phonon emission scattering length (at energies slightly above $\hbar\omega_{op}$). When this ratio is small—as it is in high electric fields—the probability of emitting an optical phonon over one oscillation period is also small. Hence, the oscillation amplitude is much smaller for high electric fields than for low. The possibility of spatial oscillations in the drift velocity and average particle energy was predicted many years ago by Price.[10] However, we have demonstrated this effect in a rigorous model of the system. In MC calculations these oscillations have recently been obtained,[11] but only in a one-dimensional quantum-wire structure. Related temporal oscillations have been obtained in the time-dependent problem when a dc electric field is turned on instantaneously.[12,13] As was stated earlier, it is very difficult to obtain the spatial oscillations from MC calculations due to the large mesh steps used in these calculations.

From Fig. 2 it is clear that, after an initial period of adjustment, the average velocity of the carriers oscillates about a constant steady-state drift velocity V_{dr}. For the fields of 50 and 100 kV/cm, there is a region of significant velocity overshoot ($\sim$25% for $F = 100$ kV/cm), before the constant drift velocity is achieved. The reason the velocity overshoot does not occur at the low fields ($\sim$10 kV/cm) observed in some MC calculations[2] is that we have neglected intervalley scattering. The very large increase in the velocity near the right side of the system is the result of the right boundary condition, which assumes no particles incident from the right. This is the so-called "anticipatory effect" observed by others using the MC technique.[14]

In Fig. 3 the average kinetic energy of the electrons is plotted as a function of z for various electric fields. The oscillations seen in these plots are associated with those

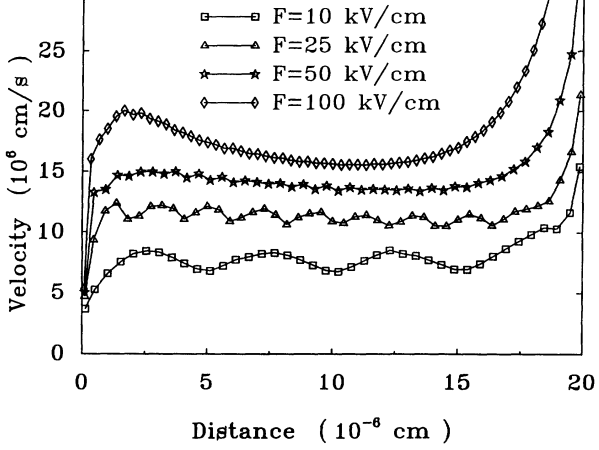

FIG. 2. Drift velocity as a function of distance for a structure length of 0.2 μm, for four different electric fields values. The symbols on the curves mark the center of the intervals used in the calculation. The oscillatory structure in the drift velocity produced by the interaction with optical phonons has a period of $L_{op} = \hbar\omega_{op}/eF$. At the highest shown field ($F = 100$ kV/cm), velocity overshoot is evident.

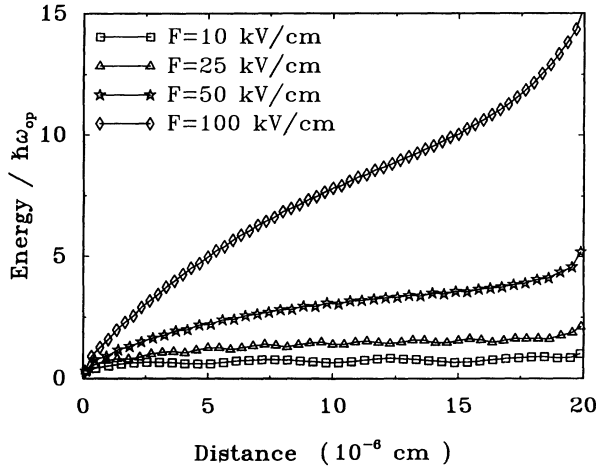

FIG. 3. Average electron energy as a function of distance for a structure length of 0.2 μm, for four different electric field values. The symbols on the curves mark the center of the intervals used in the calculation.

observed in the velocity curves of Fig. 2. As can be seen, for the larger electric fields the energy continues to increase over the entire length of the structure. For such fields, the kinetic energy of the electron can be several optical phonon energies before it has traveled one optical phonon scattering length and has a significant probability of emitting an optical phonon. As a result, not only are the electrons much hotter than in the low-field case, but they must travel much farther before a spatially constant distributions is achieved. From our results it seems that such a constant distribution has only been achieved for the two lowest field strengths shown in Fig. 3.

As a check on our results for small electric fields, we compare our solution to a low-field model of the mobility in a spatially uniform electric field. Using the same parameters as in our Boltzmann equation solution, we obtain a low-field mobility of 893 $cm^2/V\,s$. The mobilities calculated using our full solution were 950 $cm^2/V\,s$ at 5 kV/cm; 770 $cm^2/V\,s$ at 10 kV/cm; and 520 $cm^2/V\,s$ at 20 kV/cm. As is expected, the agreement between these mobilities and the low-field mobility is good at 5 kV/cm but gets progressively worse as the field strength is increased. At the higher fields of 10 and 20 kV/cm, the calculated mobilities are significantly less than the low-field value.

Having confirmed the low-field result, it is of some interest to find an approximate expression for the drift velocity in the case of the intermediate fields, when the elastic scattering length l_{el} is much smaller than L_{op}. As was shown by Shockley,[15] for high electric fields, when

$$L_{op} \ll l_{sc} , \tag{5.3}$$

the drift velocity is saturated and is given approximately by $V_{dr}=(\hbar\omega_{op}/2m)^{1/2}$. We wish to model transport in a very different field region. We consider the case when the scattering length due to absorption of optical phonons $l_{op}(E<\hbar\omega_{op})$ is much larger than the elastic scattering length l_{el}. In addition, we shall also assume that the inelastic scattering length due to acoustic phonons l_{ac}^{inel} is larger that L_{op}. This last assumption allows us to neglect the loss of electron energy to acoustic phonons. These two conditions can be expressed as

$$l_{el} \ll L_{op} \lesssim l_{ac}^{inel} . \tag{5.4}$$

In the absence of impurity scattering, l_{el} is the elastic mean free path l_{ac}^{el} due to acoustic phonons. It is well known that $l_{ac}^{inel} \cong (k_B T/2mS^2) l_{ac}^{el}$ (where S is the velocity of sound), and thus $l_{el} \ll l_{ac}^{inel}$, as we have assumed.

The approximate expression for the velocity in the absence of optical phonons, when the inequality

$$l_{el} < l_{ac}^{inel} \ll L_{op} , \tag{5.5}$$

is satisfied, has been obtained by Druyvesteyn[16] using the BTE with energy loss due to acoustic phonons taken into account (see also Ref. 15). From this work, it follows that the dependence of V_{dr} on field changes from its low-field linear behavior to a $\sqrt{F}$ law. As has been shown by Shockley, the square-root law is due to the field-induced increase in the average electron-gas temperature. As we shall show in the following, the same square-root law is expected when the condition of Eq. (5.4) is met, i.e., when acoustic phonon losses do not play any role.

If the average electron energy in the presence of an electric field is much smaller than the optical phonon energy, then the electron must travel a distance L_{op} before it can emit an optical phonon. If $L_{op} \gg l_{el}$, then the drift velocity is determined by the average time an electron takes to travel the distance L_{op} for the given elastic scattering mechanism. We consider first the case of an energy-independent elastic scattering length l_a such as is found in scattering from acoustic phonons in the quasi-elastic approximation, and take $l_{el} < L_{op}$. Let $\langle z \rangle$ be the average elastic mean free path of an electron in the direction of the electric field. The average time necessary for an electron to cover this distance is determined by the relation $\langle z \rangle = (eF/2m)t^2$. The average drift velocity is equal to

$$V_{dr} = \tfrac{1}{2}(eF/m)t = (eF\langle z \rangle/2m)^{1/2} .$$

It is not difficult to see that $\langle z \rangle = l_{el}/2$. Indeed, the probability that the electron will cover a distance r without scattering and then scatter in the interval $[r, r+dr]$ is equal to $\exp(-r/l_{el})dr/l_{el}$. If the electron moves at an angle η to the z axis, then the probability that it reaches the plane at z is given by $\exp[-z/(ul_{el})]dz/(ul_{el})$ where $u=\cos(\eta)$. If the angular distribution of electrons is close to being spherical, then the average probability that an electron reaches the plane z without scattering and scatters in the interval $z, z+dz$ is given by

$$dw(z) = \int_0^1 e^{-z/ul_{el}} \frac{du dz}{ul_{el}} . \tag{5.6}$$

Note that this expression is consistent with the form of the solution Eq. (2.9), and testifies that the scatternig free path used in Eq. (2.7) (at $\omega=0$) has the same definition as that used here. The average free path is therefore given by

$$\langle z \rangle = \int_0^\infty dz \int_0^1 du \frac{z e^{-z/ul_{el}}}{ul_{el}} = \frac{l_{el}}{2} . \tag{5.7}$$

Thus, in the case of an energy-independent scattering length, the drift velocity equals

$$V_{dr} = \left[\frac{eFl_{el}}{4m} \right]^{1/2} . \tag{5.8}$$

Figure 4 shows the dependence of V_{dr} on the electric field calculated both using Eq. (5.8) and using the steady-state value of the average velocity obtained from the exact solution of the BTE. An energy-independent elastic scattering length $l_{el}=10^{-6}$ cm (which satisfies the condition $L_{op} \geq l_{el}$ for $F \leq 50$ kV/cm) was used for both calculations. As can be seen, the two results agree qualitatively, with both showing a velocity which increases approximately as the square root of the electric field. The deviation of the BTE results from square-root behavior for electric fields greater than about 5 kV/cm. This is because, at these field strengths, a significant proportion of

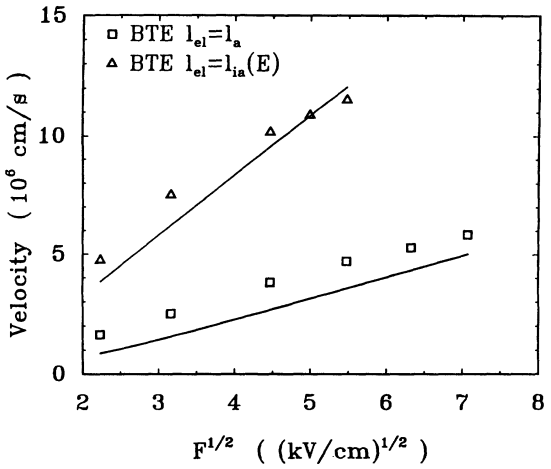

FIG. 4. Electric field (F) dependence of the average electron drift velocity for intermediate electric fields ($L_{op} \gtrsim l_{el}$), for elastic scattering lengths given by $l_{el}=l_{ia}(E) \equiv l_{ac}^{el}+l_{imp}(E)$ (triangles) and by $l_{el}=l_a=10^{-6}$ cm (squares). The solid lines are the result for the two types of elastic scattering using the phenomenological model [Eq. (5.8)].

the electrons are beginning to saturate at the Shockley value of $\sqrt{\hbar\omega_{op}/2m}$.[15] Because it is not clear without a detailed calculation what the average elastic scattering length should be in the models, we have taken this to be an adjustable parameter and set it to 4.6×10^{-6} cm. For such a choice, $l_{el}>L^{op}$ if $F>12$ kV/cm. Thus it is perhaps not surprising that the agreement of the model with the BTE data is rather poor at these higher fields.

VI. CONCLUSION

We have presented a method by which the numerical solution to the Boltzmann transport equation in arbitrary one-dimensional potentials can be obtained. Applying this method to a short interval of silicon in an electric field, we have demonstrated velocity overshoot and heating of the electrons by the electric field. In addition, oscillations in the average velocity and energy, which are associated with optical phonon emission, have been observed for a wide range of field strengths. Finally, we have proposed a simple phenomenological model of drift velocity in moderate electric fields, which is qualitatively accurate for systems where the elastic scattering is essentially independent of the energy, such as the scattering from acoustic phonons. The method used in this work is of sufficient generality and speed that it should be applicable to a wide variety of time-dependent and time-independent transport problems which are difficult to analyze using Monte Carlo techniques.

ACKNOWLEDGMENTS

One of us (M.M.D.) would like to thank the Natural Sciences and Engineering Research Council of Canada for financial support.

APPENDIX A: SCATTERING MECHANISMS

In this appendix we present the expressions for the scattering terms in the BTE. Most of the expressions are standard in the literature[17] and we include them here simply for completeness. The nonpolar optical phonon scattering length is given by

$$\frac{1}{l_{op}(E_\nu)}=\frac{e^{\beta/2}\sqrt{E_\nu-1}+e^{-\beta/2}\sqrt{E_\nu+1}}{2\sqrt{E_\nu}\,l_{op}\cosh(\beta/2)}\ , \tag{A1}$$

where

$$\frac{1}{l_{op}}=\frac{E_{op}^2 m^2\omega_{op}}{2\pi\rho S^2\hbar^3}\coth(\beta/2)\ , \tag{A2}$$

where $\beta=\hbar\omega_{op}/k_BT$ (k_B being the Boltzmann constant), ρ is the material density, S is the velocity of sound, and E_{op} the optical deformation potential. The scattering length due to acoustic phonons in the quasielastic approximation, l_{ac}^{el} is given by

$$\frac{1}{l_{ac}}=\frac{E_{ac}^2 m^2 k_B T}{\pi\rho S^2\hbar^4}\ , \tag{A3}$$

where E_{ac} is the acoustic deformation potential. The impurity scattering length $l_{imp}(E_\nu)$, as calculated via the appropriate angular average[7] of the (anisotropic) Debye-Huckel scattering cross section, is given by

$$\frac{1}{l_{imp}(E_\nu)}=\frac{\pi N_i Q^2 e^2}{2\varepsilon_0^2 E_\nu^2(\hbar\omega_{op})^2}\left[\ln(1+\beta_D)-\frac{\beta_D}{1+\beta_D}\right]\ , \tag{A4}$$

where ε_0 is the low-frequency dielectric permittivity, N_i is the impurity concentration, Q is the impurity charge,

$$\beta_D=\frac{8m\hbar\omega_{op}E_\nu}{\hbar^2}L_D^2\ , \tag{A5}$$

and L_D is the screening length which reduces to the Debye-Huckel screening length if the system is degenerate.

$$L_D=\left[\frac{\varepsilon_0 k_B T}{4\pi e^2 N_{imp}}\right]^{1/2}\ , \tag{A6}$$

where $N_{imp}=N_c F_{-1/2}(E_F/kT)$, E_F is the Fermi energy, N_c is the conduction-band effective density of states, and $F_{1/2}(x)$ is the Fermi integral of order $-\frac{1}{2}$. In this work, we ignore capture processes and set the inverse of the capture length to zero.

The coefficients of the distribution functions in the incoming scattering term of Eq. (2.4) are given by

$$A_0(E_\nu)=\frac{1}{l_{sc}(E_\nu)}\ , \tag{A7}$$

$$A_\pm(E_\nu)=\frac{e^{\pm\beta/2}\sqrt{E_\nu\pm1}}{2\sqrt{E_\nu}\,l_{op}\cosh(\beta/2)}\ . \tag{A8}$$

The relevant physical parameters used in the calculations are given in Table I.

APPENDIX B: DETAILED EXPRESSIONS

In this appendix we present explicit expressions for the kernel in Eq. (3.5) and discuss how to deal with the singularity in this kernel. The general expression for the kernel is

$$K_\nu(z,z',E_\nu)\equiv E_1\left[\frac{|z-z'|}{l_\nu^*}\right]+\theta(u_\nu^- - u_\nu^+)\left[E_1\left[\frac{z+z'-2z_\nu}{u_\nu^- l_\nu^*}\right]-E_1\left[\frac{z+z'-2z_\nu}{u_\nu^+ l_\nu^*}\right]\right]$$
$$+\theta(u_\nu^+ - u_\nu^-)\left[E_1\left[\frac{2z_{\nu+1}-z-z'}{u_\nu^+ l_\nu^*}\right]-E_1\left[\frac{2z_{\nu+1}-z-z'}{u_\nu^- l_\nu^*}\right]\right]$$
$$+\int_0^{u_\nu^m}\left[\cosh\left[\frac{z_{\nu+1}+z_\nu-z-z'}{u_\nu l_\nu^*}\right]+\exp\left[-\frac{w_\nu}{u_\nu l_\nu^*}\right]\cosh\left[\frac{z-z'}{u_\nu l_\nu^*}\right]\right]\frac{du_\nu}{u_\nu\sinh(w_\nu/u_\nu l_\nu^*)}\ , \tag{B1}$$

where $u_\nu^m\equiv\min\{u_\nu^-,u_\nu^+\}$, and

$$E_n(z)\equiv\int_1^\infty e^{-zt}t^{-n}dt=\int_0^1 e^{-z/t}t^{n-2}dt\ . \tag{B2}$$

If the potential is a monotonically increasing or decreasing function of position, then the last term in Eq. (B1) is zero and the kernel depends only upon the exponential integral functions, E_1, for which efficient numerical algorithms exist.

Because $E_1(z)$ diverges logarithmically when $z\to 0$, $K_\nu(z,z',E_\nu)$ diverges in the same way as $z'\to z$. To remove this difficulty in the integral over the kernel in Eq. (3.15), we perform the substitution

$$\int_{z_\nu}^{z_{\nu+1}}K_\nu(z,z',E_\nu)R_\nu(z',E_\nu)dz'$$
$$\equiv\int_{z_\nu}^{z_{\nu+1}}K_\nu(z,z',E_\nu)[R_\nu(z',E_\nu)-R_\nu(z,E_\nu)]dz'$$
$$+R_\nu(z,E_\nu)\int_{z_\nu}^{z_{\nu+1}}K_\nu(z,z',E_\nu)dz'\ . \tag{B3}$$

It is a simple matter to obtain an analytic expression for the last integral in Eq. (B3). When the first integral is discretized, the element where $z'=z$ is now zero and so can be omitted. Thus, the singularity no longer poses a problem.

[1] G. D. Mahan, J. Appl. Phys. **58**, 2242 (1985).

[2] See, e.g., C. Jacoboni and Paolo Lugli, *The Monte Carlo Method for Semiconductor Device Simulation* (Springer-Verlag/Wein, New York, 1989).

[3] G. A. Baraff, Phys. Rev. **133**, A26 (1964).

[4] N. N. Grigorev, I. M. Dykman, and P. M. Tomchuk, Fiz. Tverd. Tela (Leningrad) **10**, 1058 (1968) [Sov. Phys. Solid State **10**, 837 (1968)].

[5] S. Krishnamurthy, A. Sher, and A. B. Chen, Appl. Phys. Lett. **55**, 1002 (1989).

[6] H. Lin, N. Goldsman, and I. D. Mayergoyz, Solid State Electron. **35**, 33 (1992).

[7] A. Grinberg and S. Luryi, Solid State Electron. **35**, 1299 (1992).

[8] G. A. Baraff, Phys. Rev. **128**, 2057 (1962).

[9] L. V. Keldysh, Zh. Eksp. Teor. Fiz. **48**, 1692 (1965) [Sov. Phys. JEPT **21**, 1135 (1965)].

[10] P. J. Price, IBM J. Res. Dev. **3**, 191 (1959).

[11] J. P. Leburton and D. Jovanovic, Semicond. Sci. Technol. **7**, B202 (1992).

[12] A. Matulionis, J. Pozela, and A. Reklaitis, Phys. Status Solidi **31**, 83 (1975).

[13] M. Brauer, Phys. Status Solidi **81**, 147 (1977).

[14] See, e.g., C. M. Maziar *et al.*, IEEE Trans. Electron Devices **ED-32**, 783 (1985).

[15] W. Shockley, Bell Syst. Tech. J. **30**, 990 (1951).

[16] X. Druyvestyn, Physica **10**, 61 (1930).

[17] See, e.g., E. M. Conwell, *High Field Transport in Semiconductors* (Academic, New York, 1967).